# Sulfate Resistance and Microstructure Changes of Sustainable Self-Compacting Concrete Containing Micro to Nano Waste Materials

**Marwah H. Mohammed**
College of Engineering, University of Anbar, Iraq
mar21e1002@uoanbar.edu.iq (corresponding author)

**Mahmoud Khashaa Mohammed**
College of Engineering, University of Anbar, Iraq
mahmoud.mohammed@uoanbar.edu.iq

*Received: 2 July 2025 | Revised: 22 July 2025 and 4 August 2025 | Accepted: 11 August 2025*

 *DOI: https://doi.org/10.48084/etasr.13109*

## ABSTRACT

**The concrete microstructure may change the resistance of concrete to the penetration of aggressive substances from the environment into the concrete body. Incorporating micro-to-nano waste materials, such as Limestone (LS), Fly Ash (FA), Glass Powder (GP) and Kaolin (K), can modify the concrete microstructure and increase its chemical resistance. This study investigated the use of four waste material formulations with different scales in medium-strength (at the range of 25-45 MPa) sustainable Self-Compacting Concrete (SCC), and its sulfate resistance and microstructural changes were studied. Ordinary Portland cement was replaced with 40% waste materials at the microscale, and 4% at the microscale to nanoscale. The analysis of the performed tests showed that the type and scale of the cement replacement material significantly affected the durability performance of SCC under magnesium sulfate exposure. In addition to the fresh properties, the flowability improved significantly with the use of waste materials at the microscale, while the passing and segregation resistances of microscale to nanoscale waste materials improved more than microscale replacement. The tests performed showed that 4% FA demonstrated a better mechanical performance and durability in a magnesium sulfate environment.**

***Keywords-sulfate attack; sustainable self-compacting concrete; microstructure; nano; micro; waste materials***

## I. INTRODUCTION

Concrete is considered a durable material. However, the durability and integrity of concrete may be significantly affected by aggressive substances penetrating from the surrounding environment through chemical reactions. Sulfate damage is a significant factor in the deterioration of the strength of cementitious materials [1, 2]. Sulfates are present in groundwater and soil in many parts of the world [3]. Therefore, the service life of reinforced concrete structures is significantly shortened by their high susceptibility to corrosion due to the cracks caused by the sulfate attack [4, 5].

Expansion is the primary cause of concrete deterioration when exposed to sulfates. The formation of ettringite and gypsum is the main cause of concrete expansion [6]. When $Mg_2^+$ is present in the sulfate solution, the main products are gypsum and M-S-H, whereas ettringite and gypsum are more common when $Na^+$ is present [7]. The formation of ettringite within the micropores of the microstructure (e.g., C-S-H) causes the expansion and destruction of the cement paste. This has been shown through expansion tests of mortar immersed in 5% sodium sulfate ($Na_2SO_4$) and Scanning Electron Microscope (SEM) characterization [8].

Construction engineers favor SCC because of its fluidity, stability, and homogeneity [9]. SCC has the features of high cement consumption, high sand proportion, and low water-binder ratio [10]. However, the high cement content in SCC has a negative impact on the environmental sustainability, as the manufacture of cement releases significant amounts of greenhouse gases, such as $CO_2$ [11]. In addition to reducing the use of cement, replacing cement with a large amount of waste materials can enhance SCC's properties and can achieve sustainability from economic and environmental points of view [12]. Moreover, increasing the durability of SCC reduces the cost of premature repairs and reconstruction, while preserving the necessary degree of safety for a longer amount of time [13].

The alkaline nature of SCC and its interaction with sulfates leads to the shortening of the SCC's service life in sulfate-rich environments, such as groundwater, saline soil, ocean water, and contaminated water [14]. Sulfates are typically found in high-clay soils and acidic groundwater conditions, although they can also be found in the raw materials of concrete.

Therefore, concrete may be damaged under these conditions by expansion, cracking, and spalling.

The microstructure and degradation, attack mechanisms, and methods to improve the concrete under sulfate attack have been thoroughly examined [15]. Previous works have shown that various mineral materials may enhance the resistance and compactness of concrete through chemical changes and filling activity. These materials might help to inhibit the sulfate ions from penetrating concrete, and consume the calcium hydroxide in the concrete's hydration products. This can happen through secondary hydration and thus, these materials may reduce the amount of ettringite produced during the sulfate attack and enhance the concrete's resistance to corrosion. For example, the use of ground granulated blast slag and FA in concrete can increase the sulfate attack resistance [16]. The results in [17] indicate that the type of mineral additives significantly affect the durability of reinforced SCC when exposed to magnesium sulfate. Authors in [18] assessed the resistance to sulfate attack by noting the changes in the weight and strength of normal concrete after 7, 28, and 90 days of exposure to magnesium sulfate when waste glass was used. They concluded that the incorporation of waste glass increased the resistance of concrete to the sulfate attack.

Numerous studies have been conducted on the relationship between the durability and microstructural properties of high-strength SCC using waste materials. However, the studies on the relationship between the sulfate attack and changes in the microstructure properties for medium-strength sustainable SCC using waste materials are scarce. The current study focuses on the production of medium-sustainable SCC with waste material at different scales (micro and nano), as well as their relationships with the durability and microstructure of concrete. Different percentages of waste materials, namely Limestone (LS), Fly Ash (FA), Glass Powder (GP) and Kaolin (K), were used in SCC and its change in compressive strength after exposure to magnesium sulfate was explored. Qualitative and quantitative examinations of the microstructural changes of the SCC samples were also performed.

## II. MATERIALS, MIX DESIGN, AND SAMPLES PREPARATION

### A. Materials

Two types of aggregates were employed in this study: i) crushed coarse aggregate with a maximum size of 10 mm, which complies with the ASTM C33-78 criteria, and 770 kg/m$^3$ was used in all mixtures. The bulk density and specific gravity of this type of aggregate were 1.450 g/cm$^3$ and 2.35, respectively. ii) Fine aggregate natural river sand, having a bulk density of 1.63 g/cm$^3$, specific gravity of 2.65, and 850 kg/m$^3$ was used. Type I Portland cement with a specific density of 3.15 was utilized. By weight of cement, the main compounds were 10.33% $C_4A$, 27.8% $C_2S$, 6.76 % $C_3A$, and 44.6% $C_3S$ [19]. Four natural and industrial waste materials were used: LS, FA, GP, and K. They were utilized as a partial replacement of cement with a present of 0-40% at micro-scale and 0-4% at micro to nanoscale. Potable water (160 kg/m$^3$) was used as mixing water for all mixtures, with high range water reducing admixture (SP) (Master Glenium 51 (5.52 kg/m$^3$)) and Viscosity Modified Agent (VMA). This was done to achieve the required flowability, stability, and viscosity of the SCC mixtures.

### B. Waste Materials Properties

Table I displays the chemical compositions of the waste materials determined using X-ray Fluorescence (XRF). Figures 1 and 2 illustrate the XRD and SEM results of the prepared materials. The diffraction pattern of LS revealed a pure calcite phase (98.3 %) without any indication of amorphous material. In contrast, FA consisted of a glassy medium with two main crystalline phases: quartz ($SiO_2$) and mullite ($Al_6Si_2O_{13}$). For GP, the presence of a convex region at 20°-32° indicates the presence of an amorphous structure. The XRD pattern of K clay shows three intense diffraction peaks at 2θ values of 12.4°, 24.8°, and 26.6°, and a less intense peak at 36.7°. The intense peaks corresponded to kaolinite, quartz, and illite. The SEM analysis showed different shapes of micro- and micro-to-nanoparticles in all the waste materials. Angular surface texture was found at the LS particles. In contrast, the FA particles had a smooth surface texture and spherical shape. The glass particles were of varying sizes and had edges at different angles, in addition to the accumulation of smaller glass particles on the surface of the larger particles. The K grains exhibited a layered, agglomerated shape with a rough texture.

### C. Mix Design and Sample Preparation

SCC was produced using LS, FA, GP, and K at multiple length scales and in different proportions. The constituents (diameter, time ($T_{500}$), passing ability (Bj), Segregation Index (SI), and compressive strength) of the Control (Cont.) and other mixtures containing waste materials are presented in Table II.

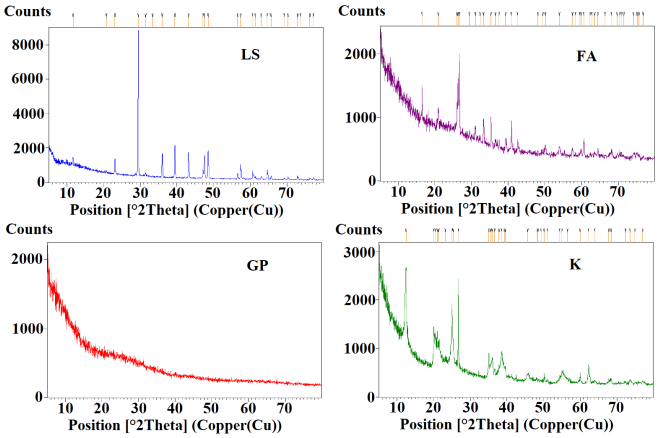


Fig. 1. XRD patterns of LS, FA, GP, and K.

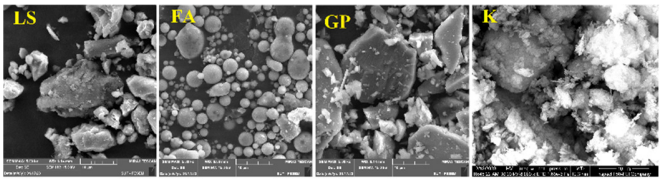


Fig. 2. SEM images of LS, FA, GP, and K.

TABLE I. MAIN CHEMICAL COMPOSITION OF WASTE MATERIALS DETECTED BY XRF

| Material | Waste type | $SiO_2$ | $Al_2O_3$ | $SO_3$ | $K_2O$ | $Na_2O$ | MgO | CaO | $Fe_2O_3$ |
|---|---|---|---|---|---|---|---|---|---|
| LS | Natural | - | - | - | - | - | - | - | - |
| GP | Industrial | 72.263 | 0.952 | 0.252 | 0.37 | 12.729 | 3.387 | 8.244 | 0.47 |
| FA | Industrial | 51.649 | 29.298 | 1.234 | 0.695 | 0.359 | 1.335 | 7.436 | 3.278 |
| K | Natural | 48.509 | 33.002 | 0.189 | 0.427 | 0.23 | 0.322 | 0.337 | 1.242 |

TABLE II. DESIGN OF THE MIXES USED IN THE EXPERIMENTS

| Material | Micro% | Micro to nano% | Cement micro ($kg/m^3$) | Cement micro to nano ($kg/m^3$) | VMA g/100 | Diameter micro (mm) | Diameter micro to nano(mm) | $T_{500}$ micro(sec) | $T_{500}$ micro to nano (sec) | Bj index micro | Bj index micro to nano | SI index micro | SI index micro to nano | St in 7 days micro MPa | St in 7 days micro to nano MPa | St in 28 days micro MPa | St in 28 days micro to nano MPa |
|---|---|---|---|---|---|---|---|---|---|---|---|---|---|---|---|---|---|
| Cont | 0 | 0 | 460 | 460 | 4.5 | 740 | 740 | 1.8 | 1.8 | 0.75 | 0.75 | 6.04 | 6.04 | 32.16 | 32.16 | 42 | 42 |
| LS | 40 | 4 | 276 | 441.6 | 4.5 | 755 | 705 | 1.2 | 2.14 | 0.95 | 0.758 | 16.2 | 4.3 | 23 | 37 | 36 | 50 |
| FA | 40 | 4 | 276 | 441.6 | 4.5 | 740 | 730 | 3.75 | 2.04 | 1.05 | 0.975 | 7.74 | 5.4 | 23 | 36 | 44 | 46 |
| GP | 40 | 4 | 276 | 441.6 | 4.5 | 737 | 730 | 3 | 2.54 | 0.77 | 1.15 | 11.14 | 2.7 | 22 | 37 | 42 | 44 |
| K | 20 | 2 | 368 | 450.8 | 0.25 | 610 | 735 | 1.7 | 1.63 | 2.72 | 1 | 2.2 | 12.04 | 32 | 30 | 38 | 49 |

## III. EXPERIMENTAL PART

### A. Sulfate Attack Tests

After a curing period of 28 days, the sulfate attack tests were implemented through wetting and drying cycles. The cycles were conducted every 3 days for a total exposure time of 56 days to magnesium sulfate, as shown in Figures 3(a) and (b). The experimental procedure was:

1. After a curing period of 28 days, the SCC samples were soaked in a 25% $MgSO_4$ solution for 3 days.
2. The SCC samples were then dried for three days.
3. After 28, 42, and 56 days of magnesium sulfate exposure, the compressive strength of the samples was tested according to BS EN 12390-3 [20], as depicted in Figure 3(c). In addition, microstructure tests were performed. The mixes containing K were excluded because they contained a higher percentage of cement than the other mixes; therefore, it was difficult to compare them with the other mixes.

Characterization of the samples was conducted as follows:

#### 1) Compressive Strength Tests

According to BS EN 12390-3 [15], the compressive strength of the samples after 28, 42, and 56 days of exposure to a 25% solution of $MgSO_4$ was tested to determine the residual compressive strength using:

$$Residual\ Compressive\ Strength\% = \frac{Compressive\ strength\ after\ the\ sulfate\ attack\ test}{Compressive\ strength\ before\ the\ sulfate\ attack\ test} \times 100\% \quad (1)$$

#### 2) XRD Tests

A Philips PW 3121 X-ray diffractometer was used to identify the chemical phases of the samples tested before and after the exposure to $MgSO_4$ solution, as displayed in Figure 4(a).

#### 3) SEM Characterization

The microscopic morphologies of the SCC samples and hydration products were examined by SEM. Figure 4(b) shows the SEM instrument, and Figure 4(c) presents the prepared SEM samples.

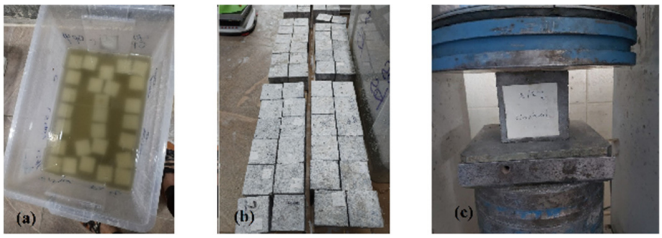


Fig. 3. The wet (a) and dry (b) cycles. (c) Testing of the compressive strength of the samples.


Fig. 4. (a) The XRD equipment, (b) the SEM instrument, and (c) the mounted SCC samples for SEM characterization.

## IV. RESULTS AND DISCUSSION

### A. Compressive Strength Change

The changes in the compressive strength after magnesium sulfate exposure of the SCC samples are shown in Figure 5. According to Figure 5, the compressive strength of all mixtures decreased with the increase of the magnesium sulfate exposure time. However, the residual strength decrease varied for the different cement replacement materials. The LS40 sample showed the highest strength loss (30%), whereas 4% FA exhibited better sulfate resistance performance (12% reduction in compressive strength) after 56 days.

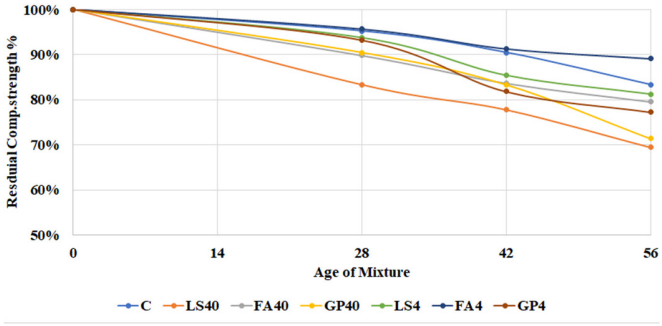


Fig. 5. The compressive strength loss of the SCC mixtures.

In this study, the mixtures at the microscale to nanoscale showed better behavior than the Cont. and SCC mixtures at the microscale. There are several possible reasons why nanoscale replacements (4% replacements) function better than their microscale mixtures (40% replacements): i) Improved particle packing: Nanoscale particles fill gaps more efficiently, lowering permeability and restricting the sulfate attack [21]. ii) Greater surface area: Nanoparticles with a higher specific surface area encourage better interfacial bonding and more extensive pozzolanic reactions. iii) Nucleation effects: A more refined microstructure results from the nucleation of the hydration products in tiny particles [22].

When comparing the type/ratios of the cement replacement materials, the FA% mixtures, especially at a ratio of 4%, showed the lowest strength change owing to the pozzolanic activity of these particles, which consume calcium hydroxide and are also able to form a denser matrix through the formation of additional C-S-H gel [23]. However, LS at the 40% replacement level showed the opposite performance to that of FA, possibly due to the formation of aluminate carbon resulting from the reaction of LS with aluminate phases present within the cement paste, which in turn can increase the instability of ettringite in sulfates [24, 25]. In contrast, the 4% LS exhibited superior performance (retaining about 75% of its compressive strength). This enhancement can be attributed to the filler effect and nucleation sites provided by the LS particles at this scale, which improved the microstructural density and reduced porosity. It can be concluded that the use of alternative materials at the microscale to nanoscale can significantly enhance the durability of SCC in aggressive sulfate attack environments, where LS, FA, and GP at microscale to nanoscale showed great promise in such applications.

### *B. XRD Results*

XRD is a suitable method for observing how the addition of sustainable materials can alter the chemical composition of concrete before magnesium sulfate exposure [26, 27], as well as the mineralogical changes after the sulfate attack. The XRD measurements showed some variations in the C-S-H gel and, in particular, in the CH content [28, 29]. With the aid of XRD, the matrix composition change was feasible. Figure 6 shows the XRD spectral changes for each type of SCC with waste materials at the microscale. At this scale, the XRD pattern shows clear changes in crystalline phases' intensities after exposure to $MgSO_4$, especially in the mixture containing 40% GP as compared to Cont. and the other samples. In contrast, the SCC with FA exhibited no clear changes. This indicates that the matrix composition of this SCC remained stable after the sulfate attack. The high reduction in the XRD intensities might propose the cautious use of GP at high levels of cement replacement in SCC exposed to aggressive sulfate attack environments. However, the use of GP at 4% microscale to nanoscale (Figure 7) reduced the changes in the cement matrix after the magnesium sulfate exposure. Thus, it is proposed to use the GP at micro to nano scale rather than microscale for SCC under high sulfate environment. For the amorphous phases, according to [30], the different forms of calcium silicate hydrate gel (CSH) would consist of amorphous phases with weak and diffuse XRD peaks under typical curing conditions. As a result, such compounds might not show up in the XRD diffractogram [30]. Thus, the Energy Dispersive X-ray Spectroscopy (EDS) analysis in the next section will clarify the CSH changes after the magnesium sulfate exposure.

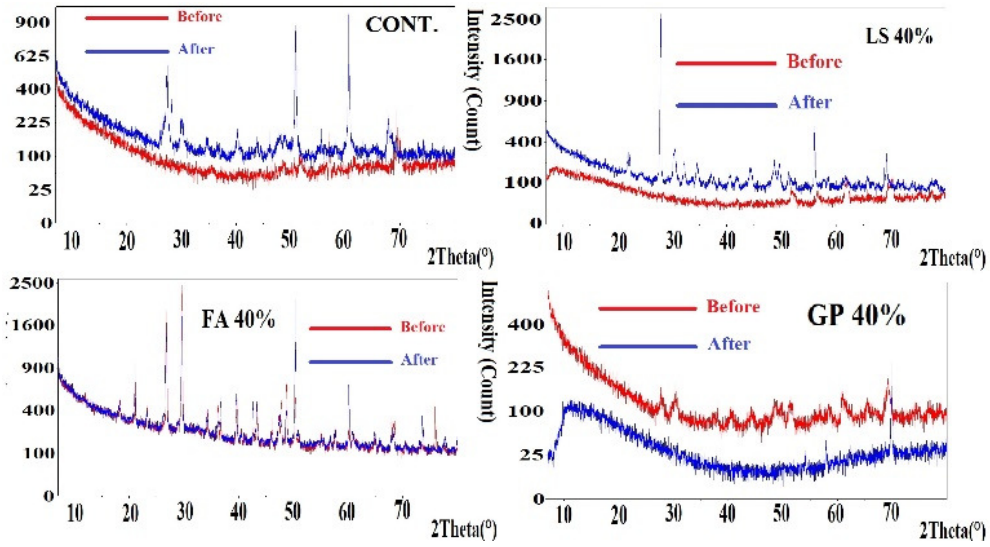


Fig. 6. The compressive strength loss of SCC mixtures.

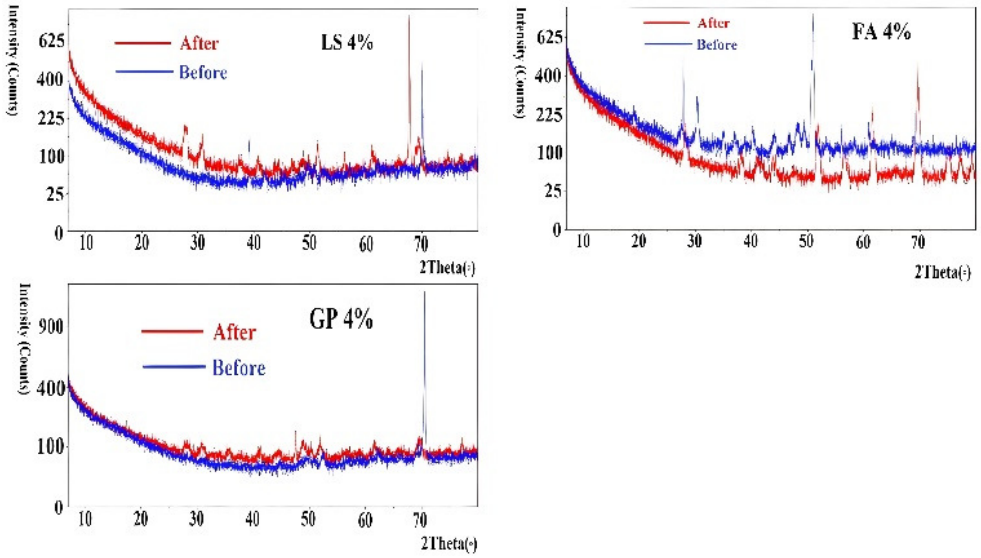


Fig. 7. The XRD charts of Cont. and CRM SCC mixtures at microscale to nanoscale.

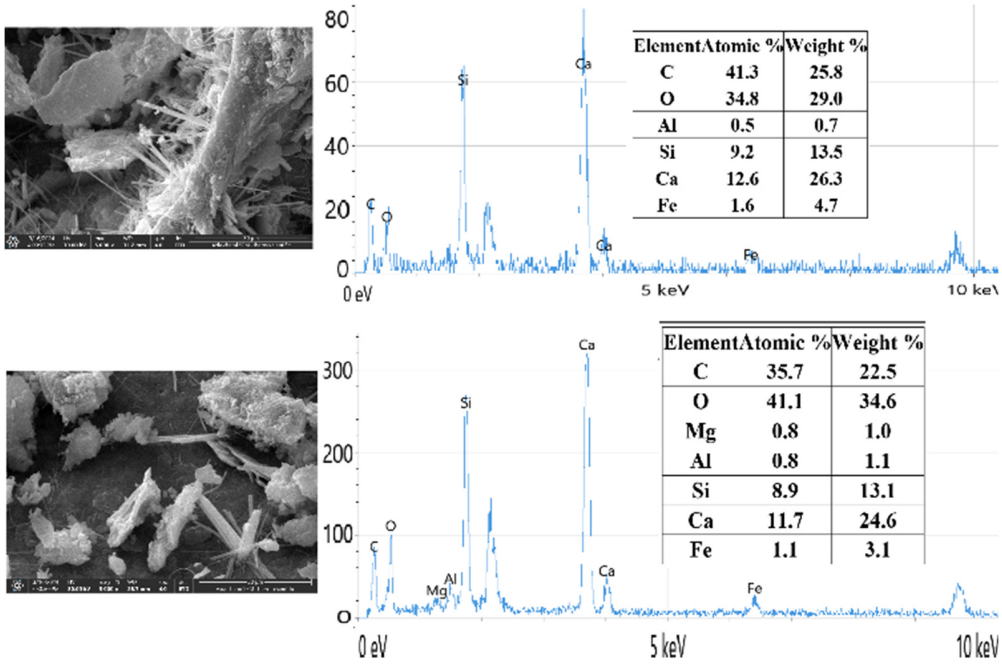


Fig. 8. SEM/EDS analysis of (a) Cont. SCC and (b) FA4% SCC after exposure to $MgSO_4$.

The presence of peaks for gypsum formation at around 29.15° 2θ for all concrete mixtures was confirmed by the superposition of the spectra. Relatively high ettringite peaks were also found, particularly at about 33.4° 2θ. Thaumasite was found in the LS 40% and GP 40%, according to the XRD patterns. The thaumasite peaks were more intense in these combinations than in the SCC Cont. and other mixtures, according to the peaks seen at 23.35°. It should be mentioned that concrete specimens exposed to magnesium sulfate at a temperature of 25±2 °C were found to contain thaumasite. Even at room temperature, small amounts of thaumasite have been shown to develop in pastes and mortars, according to earlier research [31]. Finally, the XRD results showed the presence of portlandite at around 47.5°, 50.9°, and 64.15° 2θ. Authors in [32] stated that a degree sweep of (4°-70º) utilizing a Cu-K radiation source can detect the reference peak of the CH crystalline hydration phase at this angle. The detected portlandite was weak due to the significant consumption of calcium hydroxide in the magnesium sulfate by the reaction of Cement Replacement Materials (CRMs) with $MgSO_4$ in SCC.

### *C. Microstructural and Mineralogical Changes*

The EDS pattern was used as a basis to monitor the changes occurring in the chemical composition at selected locations in the samples after the $MgSO_4$ attack. For the Cont. mix, as obtained from Figure 8(a) as an example of the analysis

performed, the analysis showed the presence of Ca and Si with a Ca/Si ratio of ≤2.5, which is an indication of the presence of C-S-H ($xCaO.ySiO_2.zH_2O$). At microscales, with the use of LS, FA, and GP, a slight decrease in Ca/Si ratio was recorded and it remained within the limit of the criteria determined for the CSH gel. This may indicate that the CSH gel was not fully decomposed after the exposure to magnesium sulfate. This can be attributed to the reaction between the hydration products and $MgSO_4$. At the microscale to nanoscale, the EDS analysis showed a C-A-S-H ($xCaO.yAl_2O_3.zSiO_2.xH_2O$) phase containing characteristic peaks for calcium, silicon, and aluminum. In most SEM images and at different locations, after the exposure to $MgSO_4$, the presence of a C-S-H phase was revealed with a Ca/Si ratio of less than 1.5, which indicates that a significant portion of the CSH gel has not been decomposed. This is true for all samples of this size and explains the reduced compressive strength of the mixes after 56 days of magnesium sulfate exposure.

According to the SEM images of FA in Figure 8(b) and the EDS analysis after the magnesium sulfate exposure, the presence of the secondary C-S-H gel was verified. This might be due to the fact that pozzolan can react with portlandite from the cement hydration reaction, which could be so useful in maintaining the best residual compressive strength for this mix, as shown in Figure 5. The analysis also exhibited the formation of this type in GP-SCC at microscale to nanoscale but in fewer manners. The binding contribution of the mineral additions, such as FA and GP, at microscale to nanoscale might play a key role in enhancing the internal structure of the cementitious matrix. The SEM and EDX analysis showed that the detection of such secondary gel in the case of micro to nano LS was not possible. However, the observed good sulfate resistance of LS4%-SCC might be a result of the enhanced filling effect of this waste material as compared to the microscale. In addition, using unreactive fillers in concrete formulation generates hydration acceleration, which increases the mechanical resistance at young ages [33].

The SEM images after magnesium sulfate exposure showed the presence of ettringite in most SCC mixes, in addition to the appearance of microcracks. This is a result of expansion resulting from the formation of gypsum and ettringite. From these images and the EDS analysis, it was concluded that the mixtures with CRMs at microscales exhibited a faster and higher deterioration rate due to $MgSO_4$ attack, whereas the micro to nano mixtures showed a lower effect due to the sulfate attack.

## V. CONCLUSIONS

Based on the results obtained from the current investigation, various conclusions can be drawn. Among the tested mixtures, the Self-Compacting Concrete (SCC) mixtures containing Fly Ash (FA) were the most effective supplementing material, particularly at 4% microscale to nanoscale replacement, where a remarkable compressive strength at 28 days (46 MPa) was recorded before its exposure to the sulfate attack. Also, it retained the highest residual strength among the other samples after the sulfate attack.

After the exposure to magnesium sulfate, all SCC microscale to nanoscale Cement Replacement Materials (CRMs) formulations showed a slight reduction in compressive strength compared to their microscale CRMs counterparts. In this respect, SCC mixtures with 4% cement replacement at the microscale to nanoscale performed better than 40% replacement at the microscale.

The microstructural and mineralogical investigations using Energy Dispersive X-ray Spectroscopy (EDS) and X-Ray Diffraction (XRD) measurements revealed that gypsum and ettringite were found in the internal structure of most SCC samples after the sulfate attack. However, the unstable structure and composition of the matrix of SCC containing GP 40% at the microscale showed that it is better to avoid using it in harsh sulfate environments. Instead, it was proposed that it should be used only at the microscale to nanoscale in such environments.

Scanning Electron Microscopy (SEM) proved that the FA mixtures at both scales, after exposure to $MgSO_4$, showed the best microstructural stability by formulating a dense C-S-H matrix that resisted the sulfate penetration. Conversely, the microscale Limestone (LS) 40% mixture exhibited the most severe internal deterioration.

After exposure to the sulfate attack, the mineralogical and microstructural changes detected by XRD, SEM, and EDS were in agreement with the macro test performed on the residual compressive strength data of most SCC mixtures at the two scales of waste materials used.

## DATA AVAILABILITY

The data of this study are available from the corresponding author upon reasonable request.

## REFERENCES

[1] R. Yin, C. Zhang, Q. Wu, B. Li, and H. Xie, "Damage on lining concrete in highway tunnels under combined sulfate and chloride attack," *Frontiers of Structural and Civil Engineering*, vol. 12, no. 3, pp. 331–340, Sep. 2018, https://doi.org/10.1007/s11709-017-0421-y.

[2] A. Campos, C. M. López, and A. Aguado, "Diffusion–reaction model for the internal sulfate attack in concrete," *Construction and Building Materials*, vol. 102, no. Part 1, pp. 531–540, Jan. 2016, https://doi.org/10.1016/j.conbuildmat.2015.10.177.

[3] S. Gao, J. Jin, G. Hu, and L. Qi, "Experimental investigation of the interface bond properties between SHCC and concrete under sulfate attack," *Construction and Building Materials*, vol. 217, pp. 651–663, Aug. 2019, https://doi.org/10.1016/j.conbuildmat.2019.05.121.

[4] L. Jiang, D. Niu, L. Yuan, and Q. Fei, "Durability of concrete under sulfate attack exposed to freeze–thaw cycles," *Cold Regions Science and Technology*, vol. 112, pp. 112–117, Apr. 2015, https://doi.org/10.1016/j.coldregions.2014.12.006.

[5] A. Merida and F. Kharchi, "Pozzolan Concrete Durability on Sulphate Attack," *Procedia Engineering*, vol. 114, pp. 832–837, Jan. 2015, https://doi.org/10.1016/j.proeng.2015.08.035.

[6] Z. Kammouna, "Enhancing the Properties of Sulfate-Resisting Cement," *Engineering, Technology & Applied Science Research*, vol. 13, no. 3, pp. 10731–10737, Jun. 2023, https://doi.org/10.48084/etasr.5827.

[7] M. N. Seifu, G. M. Kim, S. Park, H. M. Son, and S. Park, "Thermodynamic modeling of sulfate attack on carbonated Portland cement blended with blast furnace slag," *Developments in the Built Environment*, vol. 15, Oct. 2023, Art. no. 100205, https://doi.org/10.1016/j.dibe.2023.100205.

[8] C. Zhang, J. Li, M. Yu, Y. Lu, and S. Liu, "Mechanism and Performance Control Methods of Sulfate Attack on Concrete: A Review," *Materials*, vol. 17, no. 19, Jan. 2024, Art. no. 4836, https://doi.org/10.3390/ma17194836.

[9] M. Sofyan, E. Lestari, A. Amiruddin, and I. W. Kustanrika, "Selected Fresh and Hardened Self Compacting Concrete Incorporating PP Macro Fibers, Crushed Brick Aggregate, and Fly Ash," *Engineering, Technology & Applied Science Research*, vol. 15, no. 3, pp. 22698–22704, Jun. 2025, https://doi.org/10.48084/etasr.10068.

[10] R. Prakash, S. N. Raman, N. Divyah, C. Subramanian, C. Vijayaprabha, and S. Praveenkumar, "Fresh and mechanical characteristics of roselle fibre reinforced self-compacting concrete incorporating fly ash and metakaolin," *Construction and Building Materials*, vol. 290, Jul. 2021, Art. no. 123209, https://doi.org/10.1016/j.conbuildmat.2021.123209.

[11] A. Jain, S. Choudhary, R. Gupta, S. Chaudhary, and L. Gautam, "Effect of granite industry waste addition on durability properties of fly ash blended self-compacting concrete," *Construction and Building Materials*, vol. 340, Jul. 2022, Art. no. 127727, https://doi.org/10.1016/j.conbuildmat.2022.127727.

[12] N. A. Memon, M. A. Memon, N. A. Lakho, F. A. Memon, M. A. Keerio, and A. N. Memon, "A Review on Self Compacting Concrete with Cementitious Materials and Fibers," *Engineering, Technology & Applied Science Research*, vol. 8, no. 3, pp. 2969–2974, Jun. 2018, https://doi.org/10.48084/etasr.2006.

[13] P. Lehner, P. Konečný, and T. Ponikiewski, "Experimental and numerical evaluation of SCC concrete durability related to ingress of chlorides," *AIP Conference Proceedings*, vol. 1978, Jul. 2018, Art. no. 150012, https://doi.org/10.1063/1.5043803.

[14] N. Salamoni and A. B. Rohden, "Durability analysis of concrete foundations exposed to external sulfate attacks in the south of Santa Catarina, Brazil," *Journal of Building Pathology and Rehabilitation*, vol. 7, Jun. 2022, Art. no. 66, https://doi.org/10.1007/s41024-022-00205-x.

[15] Y. Wu, J. Zhu, K. Shi, X. Qiao, X. Yu, and M. Zhang, "Study on the Erosion Mechanism of the Solidified Silt Under Sulphate–Chloride Erosion," *Geotechnical and Geological Engineering*, vol. 40, no. 7, pp. 3749–3762, Jul. 2022, https://doi.org/10.1007/s10706-022-02123-8.

[16] F. Chen, J. Gao, B. Qi, D. Shen, and L. Li, "Degradation progress of concrete subject to combined sulfate-chloride attack under drying-wetting cycles and flexural loading," *Construction and Building Materials*, vol. 151, pp. 164–171, Oct. 2017, https://doi.org/10.1016/j.conbuildmat.2017.06.074.

[17] H. Siad, M. Lachemi, S. K. Bernard, M. Sahmaran, and A. Hossain, "Assessment of the long-term performance of SCC incorporating different mineral admixtures in a magnesium sulphate environment," *Construction and Building Materials*, vol. 80, pp. 141–154, Apr. 2015, https://doi.org/10.1016/j.conbuildmat.2015.01.067.

[18] M. Mathur and R. C. Chhipa, "Experimental study on durability of glass modified concrete: resistance to acid and sulphate attack," *International Journal of Advanced Technology and Engineering Exploration*, vol. 10, no. 107, pp. 1353–1367, Oct. 2023, https://doi.org/10.19101/IJATEE.2023.10101037.

[19] M. K. Mohammed, A. I. Al-Hadithi, and M. H. Mohammed, "Production and optimization of eco-efficient self compacting concrete SCC with limestone and PET," *Construction and Building Materials*, vol. 197, pp. 734–746, Feb. 2019, https://doi.org/10.1016/j.conbuildmat.2018.11.189.

[20] M. K. Mohammed, A. R. Dawson, and N. H. Thom, "Carbonation of filler typed self-compacting concrete and its impact on the microstructure by utilization of 100% $CO_2$ accelerating techniques," *Construction and Building Materials*, vol. 50, pp. 508–516, Jan. 2014, https://doi.org/10.1016/j.conbuildmat.2013.09.052.

[21] H. M. Sujay, N. A. Nair, H. Sudarsana Rao, and V. Sairam, "Experimental study on durability characteristics of composite fiber reinforced high-performance concrete incorporating nanosilica and ultra fine fly ash," *Construction and Building Materials*, vol. 262, Nov. 2020, Art. no. 120738, https://doi.org/10.1016/j.conbuildmat.2020.120738.

[22] S. Liu, T. Zhang, Y. Guo, J. Wei, and Q. Yu, "Effects of SCMs particles on the compressive strength of micro-structurally designed cement paste: Inherent characteristic effect, particle size refinement effect, and hydration effect," *Powder Technology*, vol. 330, pp. 1–11, May 2018, https://doi.org/10.1016/j.powtec.2018.01.087.

[23] Z. Guo, P. Hou, Z. Xu, J. Gao, and Y. Zhao, "Sulfate attack resistance of tricalcium silicate modified with nano-silica and supplementary cementitious materials," *Construction and Building Materials*, vol. 321, Feb. 2022, Art. no. 126332, https://doi.org/10.1016/j.conbuildmat.2022.126332.

[24] J. Bizzozero and K. L. Scrivener, "Limestone reaction in calcium aluminate cement–calcium sulfate systems," *Cement and Concrete Research*, vol. 76, pp. 159–169, Oct. 2015, https://doi.org/10.1016/j.cemconres.2015.05.019.

[25] S. Adu-Amankwah, L. Black, J. Skocek, M. Ben Haha, and M. Zajac, "Effect of sulfate additions on hydration and performance of ternary slag-limestone composite cements," *Construction and Building Materials*, vol. 164, pp. 451–462, Mar. 2018, https://doi.org/10.1016/j.conbuildmat.2017.12.165.

[26] P. Basu, B. S. Thomas, R. Chandra Gupta, and V. Agrawal, "Strength, permeation, freeze-thaw resistance, and microstructural properties of self-compacting concrete containing sandstone waste," *Journal of Cleaner Production*, vol. 305, Jul. 2021, Art. no. 127090, https://doi.org/10.1016/j.jclepro.2021.127090.

[27] A. S. Kohistani and K. Singh, "An Experimental Investigation by Utilizing Plastic Waste and Alccofine in Self-Compacting Concrete," *Indian Journal of Science and Technology*, vol. 11, no. 26, pp. 1–14, Jul. 2018, https://doi.org/10.17485/ijst/2018/v11i26/130569.

[28] R. Alyousef, O. Benjeddou, M. A. Khadimallah, A. M. Mohamed, and C. Soussi, "Study of the Effects of Marble Powder Amount on the Self-Compacting Concretes Properties by Microstructure Analysis on Cement-Marble Powder Pastes," *Advances in Civil Engineering*, vol. 2018, 2018, Art. no. 6018613, https://doi.org/10.1155/2018/6018613.

[29] P. Ghoddousi and L. Adelzade Saadabadi, "Study on hydration products by electrical resistivity for self-compacting concrete with silica fume and metakaolin," *Construction and Building Materials*, vol. 154, pp. 219–228, Nov. 2017, https://doi.org/10.1016/j.conbuildmat.2017.07.178.

[30] F. Rendell, R. Jauberthie, and M. Grantham, *Deteriorated concrete: Inspection and physicochemical analysis*. Emerald Publishing Limited, 2002.

[31] A. Skaropoulou, K. Sotiriadis, G. Kakali, and S. Tsivilis, "Use of mineral admixtures to improve the resistance of limestone cement concrete against thaumasite form of sulfate attack," *Cement and Concrete Composites*, vol. 37, pp. 267–275, Mar. 2013, https://doi.org/10.1016/j.cemconcomp.2013.01.007.

[32] S. A. Rizwan, *High Performance Mortars and Concretes Using Secondary Raw Materials: Self-compacting cementitious systems*. Saarbrucken, Germany: VDM Verlag, 2009.

[33] K. Samimi, G. R. Dehghan Kamaragi, and R. Le Roy, "Microstructure, thermal analysis and chloride penetration of self-compacting concrete under different conditions," *Magazine of Concrete Research*, vol. 71, no. 3, pp. 126–143, Mar. 2018, https://doi.org/10.1680/jmacr.17.00367.

## AUTHORS PROFILE

Marwah H Mohammed: BSc 2014, MSc 2019 in Civil Engineering from the University of Al-Anbar, Iraq. Currently, he is a PhD candidate in the Civil Engineering Department at the University of Al-Anbar.

Dr Mahmoud Khashaa Mohammed: BSc in Civil Engineering from Al-Anbar University, Iraq, MSc in Civil Engineering from the University of Technology, Iraq, PhD in Civil Engineering from the University of Birmingham in the UK. Currently, he is an assistant professor at the University of Al-Anbar.